http://www.jctjournals.com ISSN(ONLINE):2278 – 3814

Volume-14, Issue-05, May 2025
JOURNAL OF COMPUTING TECHNOLOGIES (JCT)
International Journal
Page Number: 01-05

GPR Antenna For GHz Range Using Modified Range Square Shape With Rectangular Slot Patch

Anamika Choudhary[1], Rajdeep Shrivastava[2]
[1]M.Tech Scholar, [2]Associate Professor,
[1,2]Department of Electronics and Communication Engineering *(ECE)*
[1,2]Lakshmi Narain College of Technology Excellence (LNCT-E), RGPV University, Bhopal, INDIA

***Abstract*—A This dissertation deals with the study of designing and implementation of a modified biconical antenna optimized for Ground Penetrating Radar (GPR) applications, operating effectively in the ultra-high frequency (UHF) bands. The measured results indicate that the antenna achieves excellent resonance characteristics, with a return loss (S11) of -52.27 dB, a voltage standing wave ratio (VSWR) of 1.09, and a percentage bandwidth of 142.85% in the VHF band. The antenna also demonstrates a gain of 37.75 dB, ensuring efficient subsurface penetration and signal clarity. Comparative analysis with previous antenna designs highlights significant improvements in return loss, bandwidth, and overall performance, making the modified bi-cone antenna a robust choice for GPR applications. This design advances the development of high-performance antennas for GPR systems, offering enhanced detection capabilities and improved signal fidelity in challenging subsurface environments.**
results.

***Keywords*—Resonant Frequency, Return Loss (S11), Bandwidth, Gain, Radiation Pattern.**

I. INTRODUCTION

Ground Penetrating Radar (GPR) is a specialized non-destructive electromagnetic technique widely used to detect, locate, and image buried targets or subsurface interfaces in diverse media such as soil, rock, concrete, and other visually opaque structures. Also referred to as *sub-surface radar*, *surface-penetrating radar*, *geo-radar*, or *earth-sensing radar*, GPR operates on the principle of transmitting electromagnetic waves into the ground and receiving the reflected signals from objects or contrasts in dielectric properties. These reflections are influenced primarily by the permittivity and conductivity of the medium, with conductivity controlling penetration depth and permittivity contrast enhancing target detection, while permeability plays a minor role. The recorded signals are digitally processed to extract useful information regarding the location, depth, size, and material composition of subsurface objects.

Owing to these capabilities, GPR has gained immense popularity across multiple domains: environmental studies for soil property analysis, snow and glacier thickness measurement, and contaminated land assessment; archaeological investigations for non-invasive imaging of historical sites; civil engineering applications such as bridge deck evaluation, tunnel inspection, reinforced concrete assessment, and detection of pipes and cables; defense operations for buried mine detection and underground tunnel surveillance; and geophysical studies for subsurface characterization. Its major advantages include high spatial resolution, significant penetration depth, low false alarm rate, cost-effectiveness, rapid surveying capability, and the ability to produce three-dimensional images for enhanced visualization and interpretation.

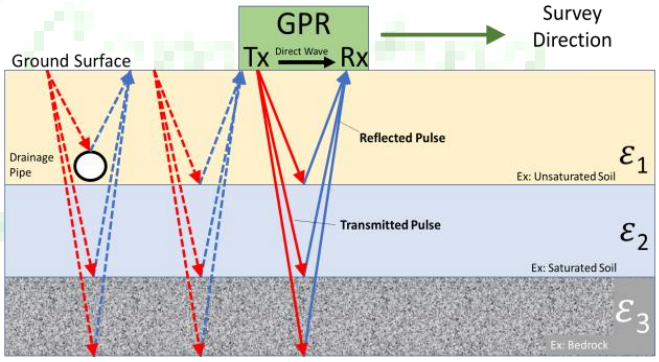

Fig. 1 : Principal of GPR

The GPR is a non-invasive geophysical method widely used for subsurface imaging and material characterization. Its efficiency and resolution largely depends on the antenna design and the operating frequency range. GHz range antennas offer higher resolution but are limited to shallow depths. The challenge lies in designing an efficient GPR antenna that balances depth penetration and resolution, while addressing the following critical issues:

- **Frequency Optimization**. Determining the appropriate frequency range to achieve the desired balance between penetration depth and resolution for specific applications,

such as archaeology, battlefield mapping, utility mapping, or geological surveys.

GPR has emerged as a critical technology for subsurface exploration and NDT across a wide range of industries, including defence, archaeology, civil engineering, utility mapping, and geological surveying. However, the effectiveness of GPR systems is often limited by the trade off between penetration depth and resolution, determined by the operating frequency of the antenna.

II. PROPOSED METHOD

In The GPR transmits UWB EM waves into the ground through an antenna. The reflected signals due to the contrasting nature of the buried targets and interfaces are received by the same antenna (mono-static mode of operation) or another antenna (bi-static mode of operation). These recorded data are stored in the digital storage device for the further processing to retrieve the vital information, i.e. depth, location and shape of the target. The processor determines the time duration taken by a pulse for the to and fro motion which is further used to determine the location of the buried object [7, 8]. The basic principle of GPR are almost same as that of ordinary radar except the fact that the medium is soil, concrete, etc. instead of air or free space. Due to the heterogeneous and stochastic behaviour of the ground, the GPR needs various extra precautions during system level designing and signal processing. A simple diagram showing the basic principles of the GPR operating is shown in Fig 2.

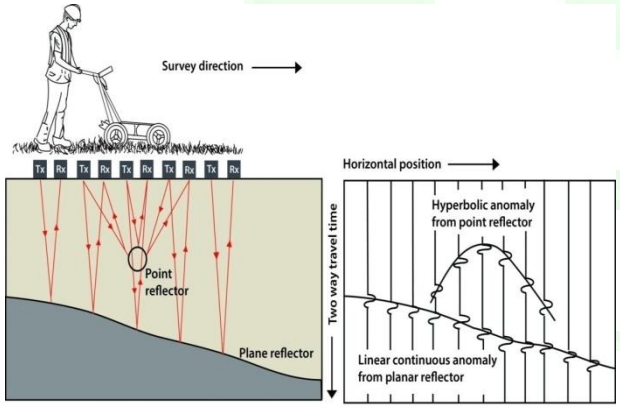

Fig. 2: Typical GPR with Basic Principal

A generic block diagram of the GPR system is as shown in Fig 2. Broadly, the GPR system can be viewed as a Radar system consists of three major components, i.e. transmitter, receiver and central processing unit. The transmitter transmits EM signal into earth surface with the help of transmitting antenna. The receiver receives the reflected back energy with the help of receiving antenna. Then, this recorded data or signal undergoes various types of RF signal processing to map the location and structure of the buried object. The outputs of the processor can be displayed in the liquid crystal display (LCD) for the interpretation by the user. The EM contrasts due to change in dielectric permittivity ϵ, electric conductivity σ, and magnetic permeability results in the reflection, transmission and refraction of the EM waves.

Governing Equations Maxwell's equations can be rewritten for the GPR applications as follows [2, 7, 10].

$$-\nabla \times \mathrm{H} + (\sigma + \mathrm{j}\,\omega\varepsilon)\mathrm{E} = -\mathrm{J} \quad (1)$$

$$\nabla \times \mathrm{E} + \mathrm{j}\omega\mu\mathrm{H} = -\mathrm{K} \quad (2)$$

where **B** is electric field vector in V/m and **H** is magnetic field vector in A/m, **D** is electric flux density vector in C/m^2 ,**B** is magnetic flux density vector in Tesla, **J** is current density vector in A/m^2 and σis charge density in C/m^3, ϵ is the dielectric permittivity which controls the velocity of the EM wave in a particular medium having dielectric constant $\boldsymbol{\varepsilon}_r$ and is give by as follows.

$$v \cong \frac{c}{\sqrt{\varepsilon_r}} \quad (3)$$

The electric conductivitycontrols the attenuation of EM wave in a particular medium and **μ** is the magnetic permeability of the medium.

The propagation of the EM waves in the GPR scenario are primarily controlled by the propagation constant, reflection coefficient and transmission coefficient. The propagation constant is a complex quantity and consists of the attenuation constant α in N /m as the real part and phase constant βin rad m as the imaginary part as given below.

$$\gamma = \sqrt{-\omega^2\mu(\varepsilon - \mathrm{j}\frac{\sigma}{\omega})} \quad (4)$$

$$\gamma = \sigma + \mathrm{j}\beta \quad (5)$$

where tan $\delta$is the loss tangent and is given by

$$\tan\delta = \frac{\sigma}{\omega\varepsilon} \quad (6)$$

The wave velocity is given by

$$\mathrm{v} = \frac{\omega}{\beta} \approx \frac{\mathrm{c}}{\sqrt{\varepsilon\mathrm{r}}} \quad (7)$$

where*c* is the velocity of light in free space and ϵr is the relative permittivity of the medium defined as follows.

$$c = \frac{1}{\sqrt{\mu_0\epsilon_0}} \quad (8)$$

$$\epsilon_r = \frac{\epsilon}{\epsilon_0} \quad (9)$$

The Reflection and Transmission Coefficients at a Boundary is givenby applying boundary conditions, i.e. continuous tangential electric field and continuous normal magnetic fields, one can find the reflection coefficient Γ and transmission coefficient T as follows.

$$\Gamma = \frac{Z_1 - Z_1}{Z_2 + Z_1} = \frac{\gamma 1 - \gamma 2}{\gamma 1 + \gamma 2} \quad (10)$$

$$\mathrm{T} = 1 + \Gamma = \frac{2Z_2}{Z_2 + Z_1} = \frac{2\gamma 1}{\gamma 1 + \gamma 2} \quad (11)$$

The main techniques and principles used in designing and optimizing bi-conical and modified micro strip antenna.

Design I: Square Shape Patch for GPR Range

For the design of GPR micro strip patch antenna we require some mathematical calculation. The square patch is easily

designed, widely used, simple to analyze and easy to manufacture. To design square patch following method is used. In the conventional procedure design of rectangular microstrip patch antenna, three essential parameters are required which are mentioned below:

- **Frequency of operation (f0),** The antenna resonance frequency must be chosen appropriately. Communication systems uses frequency range of 900 MHz to 2 GHz at different wireless frequency range. The selected resonance frequency for proposed design is 900 MHz to 2 GHz.
- **Di-electric constant of the substrate(εr),** The di-electric constant of the substrate material plays an important role in the design of the patch antenna. Dielectric constant of the substrate εr = 4.3.
- **Height of di-electric substrate (h)**.The height of the di-electric substrate must be less. In this thesis, substrate height is taken 1.6 mm.
- To design a rectangular micro-strip patch antenna according to parameters such as dielectric constant (εr), the resonance frequency (fo) and the height (h) are taken into consideration for the calculation of the length and width of the room.

Step 1: Calculation of Width (W) - For efficient radiator, the practical width which leads to a good radiation efficiency is

$$W = \frac{c}{2fo\sqrt{\frac{\varepsilon r+1}{2}}} \quad (12)$$

Where c is the speed of the free area of the light.

Step 2: Di-electric Coefficient value calculation (ε reff) The effectiveness of the di-electric constant (ε reff), using the same geometry (W h), but is surrounded by a homogeneous di-electric ε reff the effective permittivity whose value is determined by assessing the ability of the fringe field.

$$\varepsilon reff = \frac{\varepsilon r+1}{2} + \frac{\varepsilon r-1}{2}\left[1+12\frac{h}{w}\right]^{-1/2} \quad (13)$$

Step 3: Effective Length Design Equation (L eff)

$$Leff = \frac{c}{2fo\sqrt{\varepsilon reff}} \quad (14)$$

Step 4: Length Extension (ΔL) Design Equation

$$\frac{\Delta L}{h} = \frac{0.412(\varepsilon reff+0.3)(\frac{W}{h}+0.264)}{(\varepsilon reff-0.258)(\frac{W}{h}+0.8)} \quad (15)$$

Step 5: Actual Length of Patch (L) Equation The length of patch calculated by given below equation

$$L = Leff - 2\Delta L \quad (16)$$

Step 6: Ground Dimensions (Lg, Wg) Equation The broadcast line model is applicable to infinite base surfaces solely.

However, for sensible issues, it's essential to own a finite base surface. it's been shown by [6] that similar results to the finite base surface and eternity is also obtained if the scale of the bottom surface is bigger than the patch dimensions of regarding six fold the thickness of the substrate all around the edge. Therefore, for this reason, the size of the bottom surface is given by:

$$L_g = 6h + W \quad (17)$$

Step 7: Calculation of width of the micro-strip feed line Width of the micro-strip line is calculated by below eq.

$$H' = \frac{Z_0\sqrt{2(\varepsilon_r+1)}}{119.9} + \frac{1}{2}\left(\frac{\varepsilon_r-1}{\varepsilon_r+1}\right)\left(\ln\frac{\pi}{2} + \frac{1}{\varepsilon_r}\ln\frac{4}{\pi}\right) \quad (18)$$

$$\varepsilon_{eff} = \frac{\varepsilon_r+1}{2}\left[1-\frac{1}{2H'}\left(\frac{\varepsilon_r-1}{\varepsilon_r+1}\right)\left(\ln\frac{\pi}{2} + \frac{1}{\varepsilon_r}\ln\frac{4}{\pi}\right)\right]^{-2} \quad (19)$$

Where ϵr is di-electric constant, Zo is 50 ohm and h is 1.6mm.

Step 8: Calculation of length of the micro-strip feed line Free-space wavelength (λo):

$$\lambda o = c / f \quad (20)$$

III. Simulation & Result

The antenna, designed for operation in the UHF frequency ranges. These frequency bands support a variety of applications GRP antenna. Typically, GPR systems operate in a frequency range between higher frequency antennas (1-2 GHz) are generally used for shallow depth investigations (up to a few meters), such as detecting rebar in concrete structures or utility pipes in pavement. The optimized geometric dimensions, detailed in of the previous chapter, are revisited as part of the parametric study. Furthermore, the simulation results, obtained using CST Microwave Studio, demonstrate the enhanced performance of the proposed antenna compared to earlier designs, particularly in terms of S11 and VSWR.

Results Parameters

A. Return Loss (S-11)

It is the power loss in signal that is reflected due to discontinuity in transmission line, i.e when impedance matching between transmitter and receiver is not perfect. The return loss is formulated as -

$$\text{Return Loss}(S11) = -20\log_{10}\left(\frac{P_i}{P_r}\right) \quad (21)$$

Where, Pi =Incident Power ,
Pr= Reflected Power

B. Voltage Standing Wave Ratio (VSWR)

The parameter VSWR is a measure that numerically describes how well the antenna is impedance matched to the

transmission line it is connected to. VSWR stands for Voltage Standing Wave Ratio, and is also referred to as standing wave ratio (SWR).

$$VSWR = (1+\acute{\Gamma}) / (1-\acute{\Gamma}) \quad (22)$$

Where

$\acute{\Gamma}$ =Reflection coefficient Ideally, VSWR =1 if it is perfectly matched, that is no power is reflected back.

C. Bandwidth

Bandwidth is very important parameter of antenna. There are two types of bands present in antenna, wide band and narrow band. Wide band contains higher bandwidth and narrow band contains lower bandwidth.

Simple bandwidth is:

$$B.W. = (f2 - f1) \quad (23)$$

Percentage of bandwidth is:

$$B.W. \ \frac{2*(fh-fl)}{(fh+fl)} \quad (24)$$

D. Result Analysis

It is the power loss in the signal that is reflected due to discontinuity in the transmission line. As already known, when impedance matching between the transmitter and antenna is not perfect, the radiations within the substrate results into the standing waves

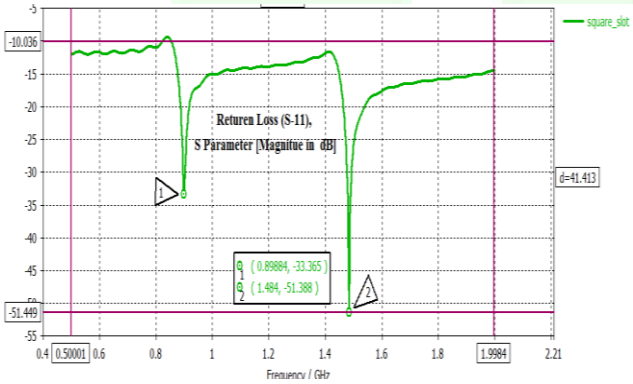

Fig. 3 : Return Loss (S-11) of proposed design II

Polar Plot The Fig. 4 shows the different form of return loss (S-11) i.e the polar form of the proposed antenna design

.

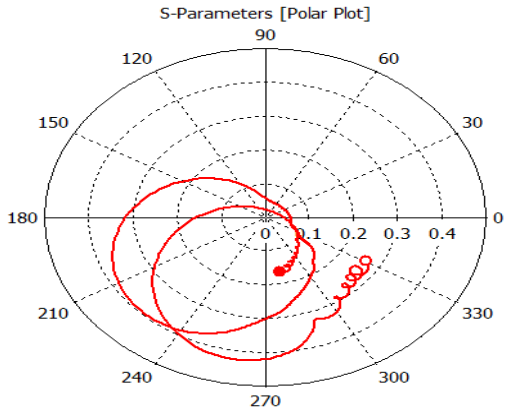

Fig. 4: Polar plot of Proposed Design

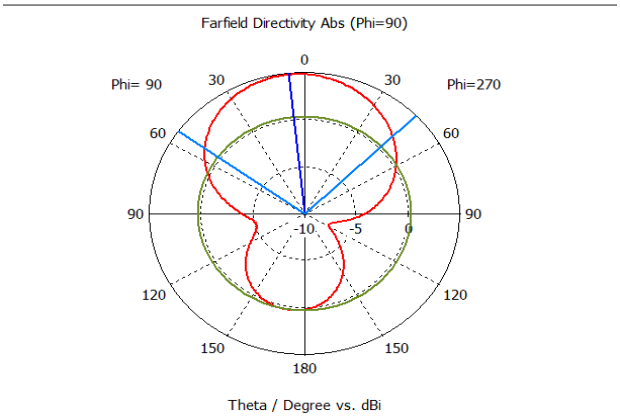

Fig. 5: 2D Graph of Far Field Pattern of the Proposed Design

IV. Conclusion

This research article presented the design, analysis, and performance evaluation of distinct antenna configurations for Ground Penetrating Radar (GPR) applications: a patch antenna and a modified micro-strip patch antenna optimized for the Ultra-High Frequency (UHF) range. The patch antenna demonstrated robustness for wideband GPR operations, making it suitable for deeper penetraton applications. Conversely, the microstrip patch antenna was specifically tailored for shallow depth exploration within the 900 MHz to 1.9 GHz range. Its compact size, low profile, and simple fabrication process make it particularly advantageous for real-world GPR use in archaeology, concrete scanning, and underground utility mapping. Notably, the microstrip patch antenna achieved an S11 value of –51.38 dB at 1.48 GHz, VSWR values consistently below across the operating band, and a wide bandwidth of nearly 120%. These results validate the effectiveness of the proposed design methodologies and their practical relevance for enhancing GPR systems.

References

[1] Shi, Xinghua, Shaolong Li, and YueMeng Yin. "A Ground Penetrating Radar Array Antenna Designed for Small Targets Detection." In Journal of Physics: Conference Series, vol. 2887, no. 1, p. 012044. IOP Publishing, 2024.

[2] Lv, Shenzhao, Chunlin Huang, Xiaoji Song, Zhihua He, and Tao Liu. "A compact ultra-wideband circular bowtie antenna for ground penetrating radar." In Journal of Physics: Conference Series, vol. 2887, no. 1, p. 012003. IOP Publishing, 2024.

[3] Gupta, Anupma, Sachin Kumar Yadav, VipanKuamr, Mohammed H. Alsharif, PeerapongUthansakul, and MonthippaUthansakul. "Enhanced breast tumor localization with DRA antenna backscattering and GPR algorithm in microwave imaging." Results in Engineering 24 (2024): 103044.

[4] Forster, Samuel JI, Anthony J. Peyton, and Frank JW Podd. "Calibration of dual-polarised antennas for air-coupled ground penetrating radar applications." Remote Sensing 16, no. 21 (2024): 4114.

[5] Kalita, Ankur, NairitBarkataki, and UtpalSarma. "Design and Optimisation of an Inverted U-Shaped Patch Antenna for Ultra-wideband Ground-Penetrating Radar Applications." (2024).
[6] Pi, Shuai, Tianhao Wang, and Jun Lin. "Directional and high-gain ultra-wideband bow-tie antenna for ground-penetrating radar applications." Remote Sensing 15, no. 14 (2023): 3522.
[7] Wagner, Samuel, AbabilHossain, Stephen Pancrazio, and Anh‐Vu Pham. "System‐based specifications for better design of ground‐penetrating radar antennas." IET Microwaves, Antennas & Propagation 17, no. 6 (2023): 478-493.
[8] Fang, Liang, Feng Yang, MaoxuanXu, and Fengyu Liu. "Research on development 3D ground penetrating radar acquisition and control technology for road underground diseases with dual-band antenna arrays." Sensors 23, no. 19 (2023): 8301.
[9] Chaabane, Abdelhalim, and Mohammed Guerroui. "Circularly polarized ultra wideband antenna with question mark-shaped patch for ground penetrating radar applications." Journal of applied research and technology 20, no. 3 (2022): 274-283.
[10] KoyadanKoroth, and Amitabha Bhattacharya. "Printed compact lens antenna Ajith for UHF band applications." Progress In Electromagnetics Research C 62 (2016): 11-22.
[11] Ajith, K. K., and Amitabha Bhattacharya. "Improved ultra-wide bandwidth bow-tie antenna with metamaterial lens for GPR applications." In Proceedings of the 15th International Conference on Ground Penetrating Radar, pp. 739-744. IEEE, 2014.
[12] Hertl, Ivo, and Michal Strycek. "UWB antennas for ground penetrating radar application." In 2007 19th International Conference on Applied Electro magnetics and Communications, pp. 1-4. IEEE, 2007.
[13] Turk, AhmetSerdar, DemetArmaganSahinkaya, M. Sezgin, and H. Nazli. "Investigation of convenient antenna designs for ultra-wide band GPR systems." In 2007 4th International Workshop on, Advanced Ground Penetrating Radar, pp. 192-196. IEEE, 2007.
[14] Busby, J. P., R. J. Cuss, M. G. Raines, and D. Beamish. "Application of ground penetrating radar to geological investigations." (2004).
[15] Wiesbeck, Werner, GrzegorzAdamiuk, and Christian Sturm. "Basic properties and design principles of UWB antennas." Proceedings of the IEEE 97, no. 2 (2009): 372-385.
[16] Tao, Yonghui, ShaohuaKan, and Gang Wang. "Ultra-wideband bow-tie antenna design." In 2010 IEEE International Conference on Ultra-Wideband, vol. 1, pp. 1-3. IEEE, 2010.
[17] Millard, S. G., A. Shaari, and J. H. Bungey. "Field pattern characteristics of GPR antennas." NDT & E International 35, no. 7 (2002): 473-482.
[18] J.-M. Friedt, "Passive cooperative targets for subsurface physical and chemical measurements: a systems perspective," IEEE Geoscience and Remote Sensing Letters, vol. 14, no. 6, pp. 821-825, 2017.
[19] W. Feng, J.-M. Friedt, Z. Hu, G. Cherniak, and M. Sato,"Wifi based imaging for gpr applications: fundamental study and experimental results," in IET international radar conference 2018, 2018, pp. 1-5.
[20] W. Feng, J.-M. Friedt, G.-M. Gwenhael, and M. Sato, "Passive radar delay and angle of arrival measurements of multiple acoustic delay lines used as passive sensors," IEEE Sensors Journal, vol. 19, no. 2, pp. 594-602, 2018.
[22] R. Chair et al., "Miniature wide-band half U-slot and half E-shaped patch antennas," IEEE Trans. Antennas Propag., vol. 53, no. 8, pp. 2645-2652, Aug. 2005.
[23] S. Pinhas, and S. Shtrikman, "Comparison between computed and measured bandwidth of quarter-wave microstrip radiators," IEEE Trans. Antennas Propag., vol. 36, pp. 1615-1616, Nov. 1988.

